Aust. J. Phys., 1988, **41**, 807–31

Lunisolar Atmospheric Tides: A New Approach

R. Brahde

Institute of Theoretical Astrophysics, University of Oslo,
P.O. Box 1029, Blindern, 0315 Oslo 3, Norway.

Abstract

In records of the atmospheric pressure in Oslo, at 60° latitude, a one-day oscillation caused by the lunisolar tide has been detected. The amplitude has a mean value of 0·17 mb. This oscillation appears during intervals when the declination of the Moon has high numerical values. When the Moon passes through the equator, the one-day oscillation disappears and only the half-day mode continues. If a maximum coincides with upper culmination, it reappears during the next fortnight at lower culmination. This means that the phase changes approximately 180° or 12^h every time the Moon crosses the equator, and this is the main reason why it has not been detected by means of traditional harmonic analysis of the atmospheric pressure oscillations. By means of the correlation between the pressure variation and the magnitude of the tidal acceleration, it was possible to separate the dynamic one-day oscillation from terms of thermal origin.

1. Introduction

Tides in the atmosphere have been observed in the past. An extensive review is found in Chapman and Lindzen (1970). Solar terms are designated S_1 and S_2 with periods of 24 and 12 hours. They are of thermal origin, and they have been demonstrated on a global scale. The dynamic tide is mainly due to the Moon, but also to the Sun. The corresponding lunar terms have been designated L_1 and L_2, representing oscillations with periods of one lunar day and one-half lunar day respectively. The term L_2 has been found in the data (Chapman and Lindzen 1970, p. 94; Haurwitz and Cowley 1969, p. 125), with amplitudes decreasing from about 0·070 mb at equatorial stations to about 0·007 mb at 60° latitude. The term L_1 has not to my knowledge been detected before.

The method used to search for lunar terms in the pressure data has been to group together data belonging to the same lunar hour, counting from the lower culmination of the Moon. Sometimes the true lunar culmination is used, but mean lunar time where a mean Moon circles the Earth at the equator has also been used extensively. In order to avoid the inaccuracies arising from the use of mean lunar time, and also to be able to compare the pressure variations with the tidal acceleration, the true Moon has been used in the following.

The formulae used in the computation are derived as follows: In Fig. 1 the Earth is represented by a sphere. The north pole is shown in the direction P, the plane of the equator is x–y, Q is the position of the observer and m marks the position of the celestial body, Sun or Moon, and also its mass. The position of m is determined

0004-9506/88/060807$03.00

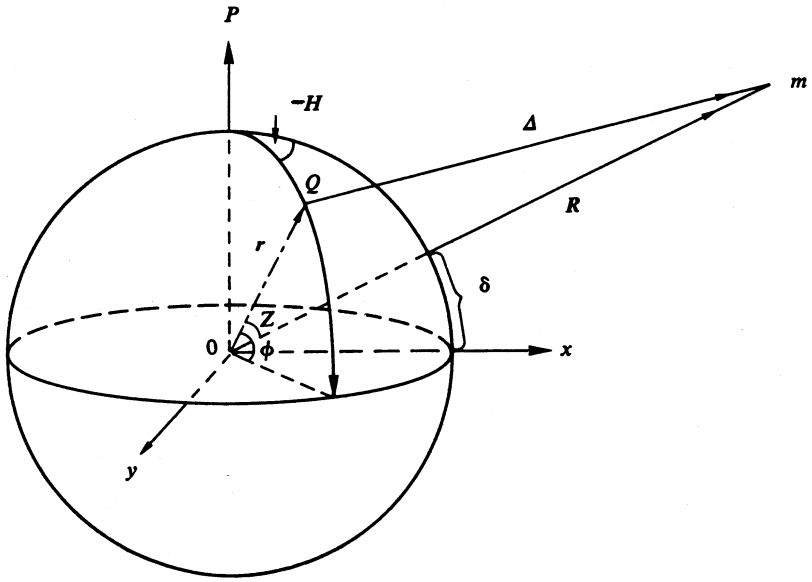

Fig. 1. The Earth as a sphere, where P is the direction to the north pole, x–y is the equatorial plane, m represents the position of the disturbing body, Moon or Sun, and Q is the position of the observer.

by the hour angle H, the declination δ and the distance R. The tidal acceleration A operating in Q equals the acceleration in Q minus the acceleration at the centre of the Earth.

With the notation of Fig. 1 we have

$$A = m(\Delta/\Delta^3 - R/R^3) = m\{(R-r)/\Delta^3 - R/R^3\}, \tag{1}$$

$$\Delta^2 = R^2\{1-2(r/R)\cos z+(r/R)^2\},$$

where z is the geocentric zenith distance of m. With

$$\Delta^{-3} = R^{-3}\{1+3(r/R)\cos z-1\cdot5(r/R)^2(1-5\cos^2 z)\},$$

we find that

$$A = mR^{-3}[R\{3(r/R)\cos z-1\cdot5(r/R)^2(1-5\cos^2 z)\} - r\{1+3(r/R)\cos z\}].$$

Division of the expression for A by the acceleration due to the gravity of the Earth, M/r^2 (where M is the mass of the Earth), introduction of the parallax of the Moon or Sun by $\sin\Pi = r/R$, and separation into a vertical V and a horizontal W component yields

$$V = (m/M)\sin^3\Pi\{-1+3\cos^2 z - \sin\Pi\,1\cdot5\cos z(3-5\cos^2 z)\},$$

$$W = (m/M)\sin^3\Pi\sin z\{3\cos z - \sin\Pi\,1\cdot5(1-5\cos^2 z)\}. \tag{2}$$

The zenith distance z is computed from

$$\cos z = \sin\phi \sin\delta + \cos\phi \cos\delta \cos H, \tag{3}$$

where ϕ is the latitude of the station. The terms included in (2) are sufficient to produce results with an accuracy of 10^{-3}.

From the theory of the Moon and Sun (see Meeus 1962) the positions of the two bodies were computed to an accuracy of 1 arcminute for every half-hour through the period covered by the data series. We note that only geocentric values are needed. As regards the vertical components the two values of solar and lunar origin are summed. However, for the horizontal components they must be further separated into two components, for the north–south and the east–west directions. By considering only the principal terms in (2), we have $V \propto 3\cos^2 z - 1$ and $W \propto 3 \sin z \cos z$, and the total acceleration becomes proportional to $(3\cos^2 z + 1)^{\frac{1}{2}}$. Also the principal term in the potential is proportional to $(1 - 3\cos^2 z)$. Consequently, the rapidly changing zenith distance enters the expressions in a similar way to the vertical component V. For these reasons the vertical component V will be used in the search for a possible connection between the tidal acceleration and variations in the air pressure.

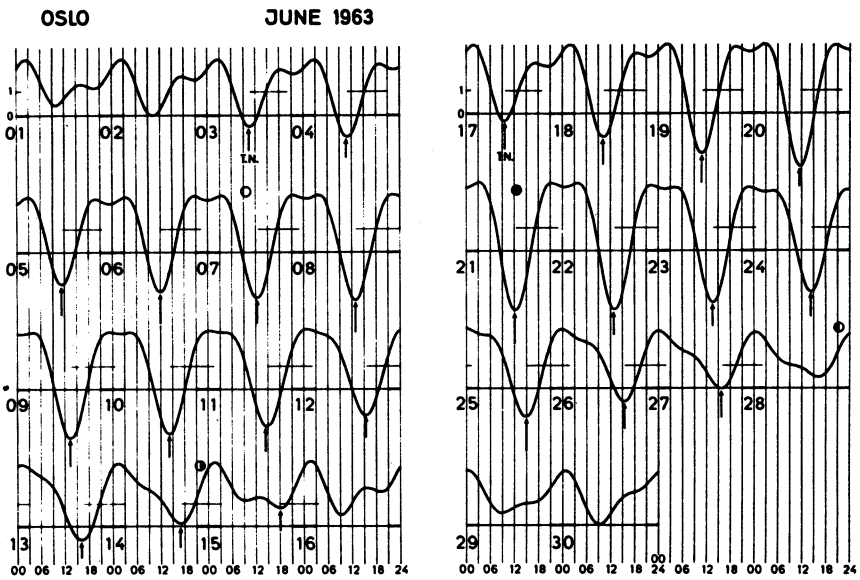

Fig. 2. Computed values of the vertical component of the tidal acceleration of Moon + Sun (multiplied by -10^7) for June 1963 in Oslo. T.N. is the moment of the principal maxima (minima of the curve). The horizontal lines following indicate the intervals when the acceleration is decreasing to the next minimum.

In Fig. 2 the computed curve for V is shown during June 1963. Apart from a scale factor of 10^7, the curve has been multiplied by -1, and therefore the minima of the curve represent maxima in V, or the curve shows the variation in gravity. The phases of the Moon are shown, and in this summer situation the one-day variation is prominent around new and full Moon, while the half-day variation manifests itself

with shallow minima in between. This is easy to explain. At upper culmination the zenith distance is $z_u = \phi - \delta$, whereas at lower culmination it is $z_l = 180° - (\phi + \delta)$. This means that

$$\cos z_u / \cos z_l = \cos(\phi - \delta) / \cos(\phi + \delta). \tag{4}$$

With the latitude $\phi = 60°$ this results in close to obliteration of the half-day oscillations when the declination has high numerical values. If δ_0 is the maximum declination of the Moon, it will change in the course of half a month from $+\delta_0$ to $-\delta_0$. Therefore, the principal and secondary maxima will change position relative to the time on a clock showing lunar time, meaning that in harmonic analysis where the data from corresponding lunar hours are grouped together, a jump of one-half lunar day will occur twice a month. This means that, whereas a half-day oscillation can be found by the method, a one-day term cannot. However, the half-day term is also present. In Fig. 2 it is seen that in between the larger one-day oscillations some days when only the shorter period occurs are found.

The combination of the lunar and solar terms also complicates the picture. For instance at equinoxes the full and new Moon occur when the declination of the Moon is close to zero, and it is seen from formula (4) that the combined effect of Sun and Moon will produce maxima twice a day with nearly the same magnitude. In equatorial regions this is different. With $\phi = 0$ in (4) it is seen that only the half-day oscillation can be present.

Consequently, a one-day lunisolar tide in the atmosphere comes into existence only at high latitudes, north or south. Another complication becomes apparent by a study of Fig. 2. The principal maxima (minima in the curve) on the 7th when the Moon is full, and on the 21st when it is new, occur close to the same time of day, at noon. Therefore the thermal tide, caused by the insolation could be mixed up with the one-day dynamical tide during some days each month.

The Norwegian Meteorological Institute provided measurements of the air pressure observed at Oslo (Blindern) every 2 hours during the 21 year period 1957–77. In the present investigation measurements for the 13 years 1957–67, 1969 and 1977 have been used. The years 1968 and 1970–76 were omitted solely because the data were difficult to read as the two first digits were not always recorded.

2. Gradient of the Pressure

In the search for a one-day pressure wave we concentrate on the gradient, and we need a method which enables us to remove the much larger variations caused by the weather, and also short-period variations which would be noise. Several methods were tried, but only the following survived the test in Section 6.

We select 25 observed values, covering 50 hours and determine the coefficients in a Fourier series:

$$a_k = \frac{2}{n} \sum_{j=1}^{n} Y_j \cos\left(\frac{2\pi}{n}(j-1)k\right), \qquad b_k = \frac{2}{n} \sum_{j=1}^{n} Y_j \sin\left(\frac{2\pi}{n}(j-1)k\right),$$

$$a_0 = \frac{1}{n} \sum_{j=1}^{n} Y_j,$$

where $n = 25$, $k = 1, 2, \ldots, 12$, and Y_j are the 25 observed values. Then the function

$$Z_i = a_0 + \sum_{j=1}^{m} \left\{ a_j \cos\left(\frac{2\pi}{n}(i-1)j\right) + b_j \sin\left(\frac{2\pi}{n}(i-1)j\right)\right\} \tag{5}$$

will reproduce the values Y_i exactly if we choose $m = 12$, i.e. we use 12 sine and 12 cosine terms. But if, for instance, only the first eight terms are used by putting $m = 8$, periods with duration 50/9, 50/10, 50/11 and 50/12 hours will be omitted, and the function Z_i will represent a smoothed curve through the data. Then, Z_i will contain periods of duration between 50 and 6·25 hours, if they are present in the data. The standard deviation of the observed values from this curve is computed from

$$\sigma = \left(\sum_{i=1}^{25} (Y_i - Z_i)^2/24\right)^{\frac{1}{2}},$$

and the value of σ will be used as a measure of the noise. The gradient could be found by derivation of (5), but in doing so, weather fluctuations with periods of 50^h could still be included. They can be removed, however, by omitting the term $j = 1$. Consequently, we get the following formula for the gradient, valid for point i:

$$Z_i' = \sum_{j=2}^{8} \left\{ -a_j \sin\left(\frac{2\pi}{25}(i-1)j\right) + b_j \cos\left(\frac{2\pi}{25}(i-1)j\right)\right\} \frac{2\pi}{25} j. \tag{6}$$

This gradient can be computed for every observed datapoint, but actually it will be needed to determine the gradient between the regular 2^h intervals. In order to do this the 25 points are selected in a way which places the central points, numbers 12, 13 and 14, close to the actual time. Then linear interpolation between Z_{12}' and Z_{13}' or between Z_{13}' and Z_{14}' defines the gradient of the pressure at this moment.

In Fig. 3 the result of the procedure is shown for the two selected cases (*a*) in July 1960 and (*b*) in July 1977. The function Z_i is shown by the curves and the crosses represent the observed data Y_i. In (*a*) the noise is small, only 0·08 mb, but in (*b*) it is 0·40 mb. Here (and in Fig. 2) a moment T.N. is indicated. This is the time when the tidal acceleration has a principal maximum and is designated by 'tidal noon'. In (*a*) the gradient has been determined at a time T.N. minus 4^h and in (*b*) at a moment T.N. plus 4^h. The arrows show the direction of the gradient. In (*a*) the gradient follows the slope of curve Z_i, but in (*b*) the gradient is positive whereas the slope of the curve is negative. The reason for this apparent discrepancy is the fact that the curve includes the long period of 50^h which was omitted in the computation of the gradient.

3. Gradient of the Pressure and the Tidal Acceleration

In the classical search for an atmospheric tidal wave (see Chapman and Lindzen 1970) the data have been arranged according to a time measure of one lunar day, or 1·03505 mean solar days. This so-called mean lunar clock can differ from a true lunar

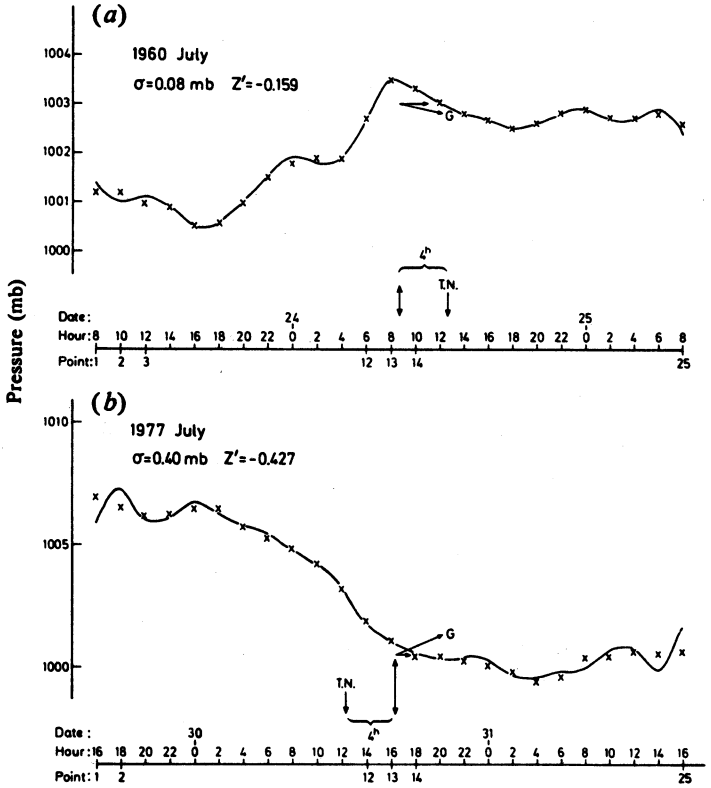

Fig. 3. Observed pressure (crosses) where the curves show the trigonometric interpolation based upon 25 observed values, including periods between 50^h and $6{\cdot}25^h$. The arrows marked G show the direction of the tangent when the 50^h period is excluded.

clock by more than one hour. The Sun is also important, even if the Moon exerts a pull 2·18 times greater when the mean distances are considered. The importance of the zenith distance which indeed is the most significant factor regarding the magnitude of the acceleration, is difficult to include in a treatment by harmonic analysis. Also, as we have already seen, the jumps between the principal and the secondary maxima will blur the traces of a one-day oscillation. Therefore, the computed curves including the vertical components of the lunar and solar tide are the basis for the comparison with the observed pressure.

From the starting points T.N. where the principal maxima take place, we could count lunar mean hours centred at T.N. However, it is preferable to use mean solar hours grouped from -14^h to $+14^h$ around T.N. in steps of 2 hours. In Fig. 2 where the moments T.N. are marked, they are followed by a horizontal line where the acceleration is decreasing after each principal maximum to the next minimum. The change of the acceleration during this interval will be used as a measure of the 'magnitude'. In order to be able to concentrate on the one-day oscillation, the

data have been omitted when the interval between two computed minima becomes shorter than 16 hours.

Consequently, the data have been sampled, and actually 69% of the total dataset has been used. In Fig. 2 for instance, the periods from the 1st to the 3rd and from the 29th to the 31st have been omitted. But in searching for the thermal effect, where the mean solar day is the basis, the complete set has been used. Ruled by the tidal clock the behaviour of the pressure gradient through a 'tidal day' has been investigated. The results from corresponding tidal hours have been grouped together and by statistical methods the variation of the pressure gradient has been found. In addition, the correlation between the gradient and the 'magnitude' of the acceleration will also be determined, the latter being unaltered during one tidal day.

4. Statistics

The data were divided into 13 groups, one for each year. The gradient of the pressure was determined at the times T.N. -14^h, T.N. -12^h, ..., T.N. $+14^h$. In each particular case the noise was determined, defined by the standard deviation of 25 points from the function Z_i of formula (5). During the tests to follow, it was found that this noise limit could be set to 0·4 mb. The magnitude of the acceleration was also noted, this being the same for each tidal day, in order to find the correlation with the gradients determined at every phase value, -14^h, -12^h, ..., $+14^h$. Mean values of all the scans during each year were formed, and finally the grand means including all of the 13 years. The uncertainty was determined from the differences between the yearly mean values and the grand mean. In Fig. 4*a* the resulting curve is seen, with error bars showing the uncertainty. The mean dynamical contribution to the pressure has been designated by $\bar{D}(\nu)$, where ν is an index which takes the values $1, 2, \ldots, 15$ corresponding to the tidal phase -14^h, -12^h, ..., $+14^h$. We see how the mean gradient $\bar{D}'(\nu)$ varies during the tidal day between the limits $\pm 0{\cdot}1$ mb. Later it will be shown that integration results in values of $\bar{D}$ between the limits $\pm 0{\cdot}17$ mb with still greater extreme variations.

Continuing the argument that it would be impossible to register this effect using a mean lunar clock instead of the tidal clock, the same program was run again with the same methods as before, but this time the mean lunar day was used and the results were grouped around the time of upper culmination of the Moon. In this case no sampling was needed. Except for the exclusion of data because of noise, the whole set was used. Fig. 4*b* shows the result. The error bars indicate that what remains of an oscillation is insignificant, or possibly a trace of the half-day oscillation with much smaller amplitude may be present.

In Fig. 4*c* another variation is shown. A period of duration $1^d.017525$ or the mean value of the solar and lunar days was formed. There is no physical reason to expect a result, and it was performed in order to determine the magnitude of eventual statistical fluctuations. The dashed curve with circles shows the result with a period of $1^d.07354$, which is Chapman's period L_1 (Malin and Chapman 1970, p. 17). The two curves show small and insignificant variations.

Finally, a period of exactly 24 hours was introduced and the result is seen in Fig. 4*d*. This curve represents the mean gradient of the thermal effect, and therefore this has been indicated by the designation $\bar{T}'(\nu)$. In this case the index ν runs from

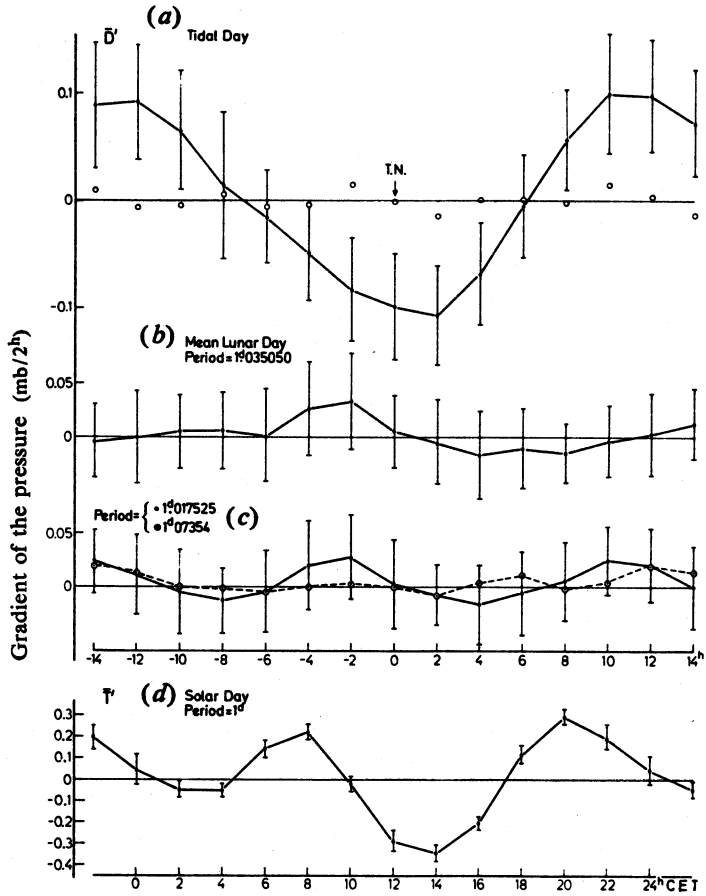

Fig. 4. Mean gradient of the pressure: (*a*) Distributed through a 'tidal day'. [Circles show the result when a series $1013 + R(t)$ is used as the data, where $R(t)$ is a series of random numbers in the range $\pm 0{\cdot}5$ mb.] (*b*) Distributed according to a mean lunar clock, where 0 is the upper culmination of the mean Moon. (*c*) Grouped according to a period between the mean lunar and the mean solar day. Circles and the dashed curve show a similar result with Chapman's period $L_1 = 1^{d}.07354$. (*d*) Grouped according to mean solar time. CET is Central European time. Note that the vertical scale is a factor of 5 larger than with (*a*), (*b*) and (*c*).

1 to 13 and corresponds to $0^h, 2^h, \ldots, 24^h$ CET (Central European time). We find two maxima, the maximum at 8^h rises to $0{\cdot}24$ mb/2^h, the minimum at 14^h falls to $-0{\cdot}34$, and the maximum at 20^h reaches $0{\cdot}28$ mb/2^h. We conclude that the thermal effect is the largest. Next comes the dynamical effect, and neither a period of one mean lunar day, nor Chapman's period L_1, can be used to detect the one-day variations. The thermal effect will depend upon the time of year, and this will be discussed in Section 8, but first the function $D(t)$ will be constructed where t is an index which marks every 2^h throughout the year.

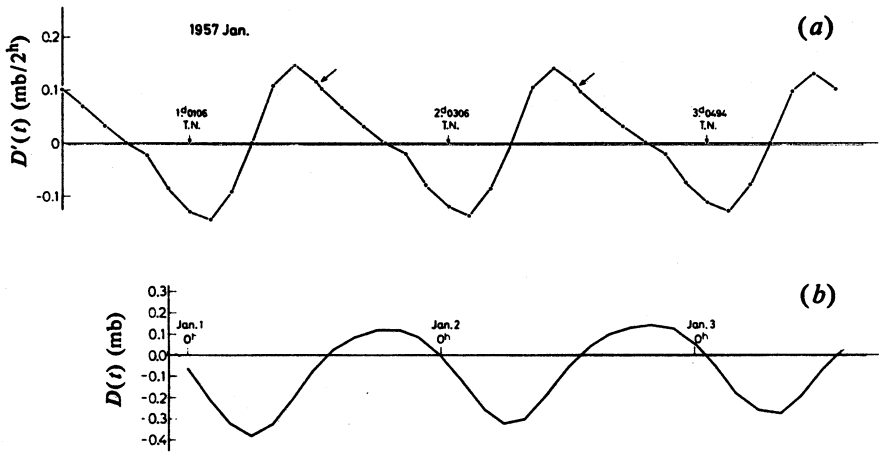

Fig. 5. The integration procedure: (*a*) Gradient of the pressure $D'(t)$ during the first days of January 1957, produced by means of the regression coefficient with respect to the magnitude of the tidal acceleration. (*b*) Integrated dynamic pressure variation $D(t)$.

5. Dynamic Atmospheric Tide

In the statistics for every tidal 2^h mark the correlation was determined between the pressure gradient and the magnitude of the acceleration. Apart from the correlation coefficient, the regression coefficient A_x in the expression $Y = A_x X$ was also found, where Y represents the pressure gradient and X the magnitude. By the magnitude we mean the difference between the maximum value at tidal noon and the minimum value 9–10 hours later. It becomes a measure of the strength of the tide on the particular day.

The correlation and regression coefficients become functions of the tidal hour. Therefore, the grand means of A_x can be used to reconstruct the function $D'(t)$. Here A_x is a function of tidal phase, and the magnitude of the acceleration is known for every tidal day. Therefore by means of the regression equation, the gradient $D'(t)$, where t is the time measure through the complete dataset, can be found except of course for the time intervals which were omitted in the sampling procedure. In order to be able to integrate $D'(t)$ we had to define $D'(t) = 0$ for every value falling in these intervals. In the procedure only the phase values T.N. -12^h to T.N. $+12^h$ were used because this is sufficient to cover an uninterrupted time scale.

In Fig. 5*a* the method is demonstrated for the first days of January 1957. Note that the curves for the individual days are replicas of each other, apart from a diminishing scale because of the diminishing magnitude of the acceleration. The first T.N. at $1^d.0106$ takes place close to lower culmination of the Moon. One hour later the Moon was new. The time measure is CET. Joints between the adjacent tidal days are marked by arrows. As a preparation for the integration of $D'(t)$, values at $0^h, 2^h, ..., 22^h$ are interpolated. Then the integration is performed by means of the trapezoidal formula. A slow monotonous variation caused by the effect that the pressure was increasing by 0·80 mb from lunar phase new/full to first/third quarter had also to be subtracted. (This is a fact of the present data, but seems to be without statistical significance.) The series $D(t)$ obtained in this way is consequently based upon:

(1) the mean pressure gradient $\bar{D}'(\nu)$ which was found by arranging the individual values in the scheme of tidal hours; and

(2) the regression between these values and the magnitude of the tidal acceleration.

Fig. 5*b* shows the result of the integration for the first days of January 1957. On the 1st of January the amplitude is 0·25 mb.

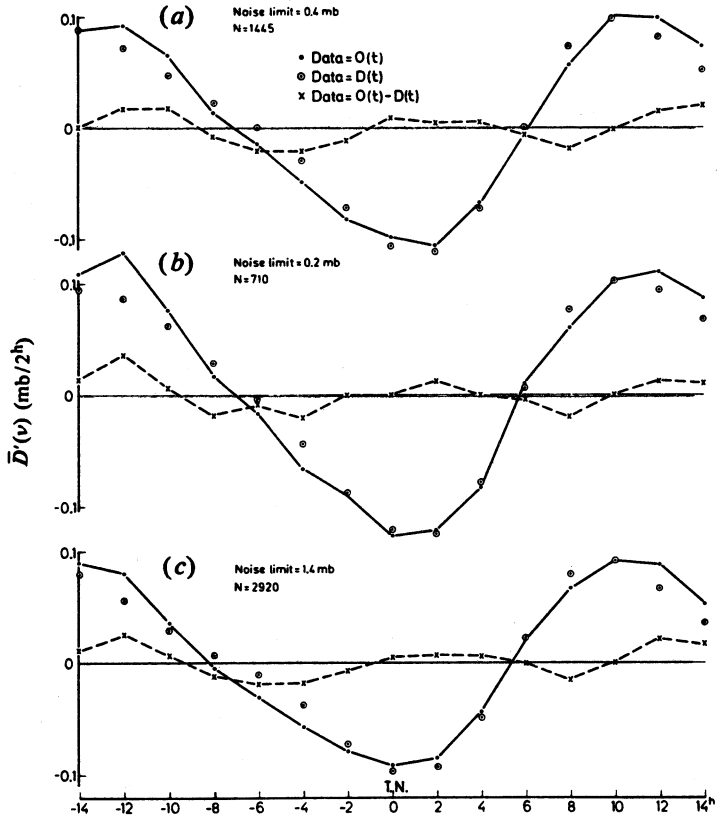

Fig. 6. Mean dynamic gradient $\bar{D}'(\nu)$ shown for three values of the noise limit: (*a*) 0·4, (*b*) 0·2 and (*c*) 1·4 mb/2^h. The solid curves were obtained with the original data, the circles with $D(t)$, and the crosses with $O(t) - D(t)$ as the data

6. Crucial Test of the Method

The reconstructed dynamical contribution to the pressure variation $D(t)$ can now be used to test the method. The program which produced the mean function $\bar{D}'(\nu)$ shown in Fig. 4*a* can be run again, but this time with the series $D(t)$ as the data instead of the observed series $O(t)$. In Fig. 6 the result is shown with three values for the noise limit (*a*) 0·4, (*b*) 0·2 and (*c*) 1·4 mb/2^h. The solid curves are obtained with the original data and the circles are the results with $D(t)$ as the data. In all cases the differences between the circles and the solid curves are small, about 0·015 mb/2^h, which is satisfactory in view of the fact that the observed pressure was noted to a

precision of 0·1 mb. However, the number of observations which is the basis of each point in Fig. 6 varies from 1445 in (*a*) to 710 in (*b*) and 2920 in (*c*), which is a natural consequence of the varying noise limit. If the noise limit is disregarded we end up with 3086 observations for each point, but in this case the test shows unacceptable differences. Therefore, a noise limit which excludes data from days with too much noise is needed. Fig. 6 demonstrates that a noise limit of up to 1·4 mb is sufficient. Nevertheless, the noise limit 0·4 mb where 47% of the available data is used was chosen because of the higher correlation coefficient with the magnitude of the acceleration, as discussed in the following.

At this point we mention that in a first attempt to determine the dynamical one-day oscillations we used a combination of straight lines adapted to the observed values by the method of least squares. Testing the result statistically revealed that the method itself produced an amplification of the effect. Then polynoms of the 2nd and 3rd degree were tried, but this time the test showed a reduction. Finally, the Fourier filtering method used here seems to be a good solution to the problem of sorting out small systematic oscillations from a dataset with considerably larger noise.

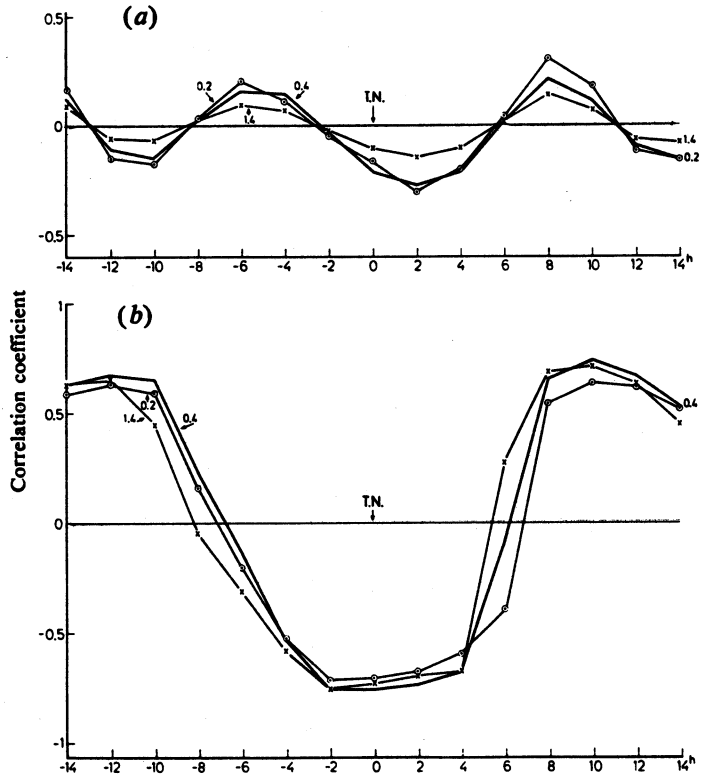

Fig. 7. Correlation coefficient between the pressure gradient and the magnitude of the tidal acceleration from the three noise limits 0·2, 0·4 and 1·4 mb: (*a*) original data used and (*b*) series $D(t)$ used as the data.

The test can also be used on the correlation coefficient between the pressure gradient and the magnitude of the acceleration. In Fig. 7*a* the original data were used and the three curves again represent cases with noise limits of 0·2, 0·4 and 1·4 mb. During

the tidal day the correlation coefficient varies between the limits $\pm 0{\cdot}30$ for noise limit $0{\cdot}2$, between $\pm 0{\cdot}14$ for noise limit $1{\cdot}4$, and between $+0{\cdot}20$ and $-0{\cdot}28$ when the noise limit of $0{\cdot}4$ mb is chosen. This supplies an argument as to why we proceed using the noise limit $0{\cdot}4$ and not $1{\cdot}4$ in the following.

Fig. 7*b* shows a similar result when the series $D(t)$ is used instead of the observed values. The correlation coefficient is considerably higher, varying between the limits $\pm 0{\cdot}75$, and it is also easier to understand the shape of the curve. There is a high positive correlation at phase -14^h to -10^h, where the gradient has positive values, then it decreases to marked negative values at -2^h to $+4^h$, where the gradient is negative, and again to positive values from $+6^h$, exactly as would be expected for a tidal wave. The more complicated picture in Fig. 7*a*, however, shows that the original data also contain information which is not of dynamic origin. Of course, this is the thermal effect which for some days each month follows the tidal day.

The simplified picture is encouraging. Not only has the correlation increased to higher extremal values of $\pm 0{\cdot}75$, but the shape of the curve indicates that the effect must be of dynamic origin. However, still another test can be performed. From the observed pressure series $O(t)$ the series $D(t)$ can be subtracted, and this new series can be used as data in the program. The result is seen in Fig. 6, where crosses connected with the dashed curves show the resulting mean gradient of the amended pressure. The amplitude of these curves is small, and if the result is significant it may indicate a residual half-day oscillation.

A final test on the validity of the results concerns the question whether it is possible to explain the dynamic pressure variation as a statistical oscillation. It has already been shown in Fig. 4*c* that a period between the lunar and the solar day resulted in a gradient $\bar{D}'(\nu)$ which is small and insignificant. In addition, the stochastic dataset $1013 + R(t)$ was constructed, where $R(t)$ is a series of random numbers in the interval $\pm 0{\cdot}5$ mb. In the construction of $R(t)$, Table 26.11 of Abramowitz and Stegun (1964) was used. The five-digit numbers were separated into five one-digit numbers, giving a series of numbers between 0 and 9 with 12500 members. This was not enough to cover the datapoints consisting of 56964 observations. Therefore, the series was counted backwards and then forwards again to obtain a series of 62500 numbers. The repetition involved should not be of any consequence as it does not repeat itself at the same time of the year, month, day or hour. From each number, $4{\cdot}5$ was subtracted and the result was divided by 9, thus resulting in additions to the constant pressure in the range $+0{\cdot}5$ to $-0{\cdot}5$ mb. In Fig. 4*a* the circles indicate the results in the process of determining $\bar{D}'(\nu)$. The same test on the determination of $\bar{T}'(\nu)$ gave a similar result, the numerical values being smaller than $0{\cdot}01$ mb/2^h.

7. Dynamic Mean Pressure Variation

So far the gradient of the pressure has been discussed, its connection with the tidal acceleration found, and the dynamical part $D(t)$ produced. The mean oscillation can be found in two possible ways. Either the series $D(t)$ may be arranged according to tidal phase and the mean values formed, or we can integrate the mean gradient $\bar{D}'(\nu)$ which was determined directly from the pressure data. In the latter procedure a trigonometric interpolation formula can be used to represent the mean gradient, and then the integration is straightforward. Fourier coefficients a_k and b_k based on

the 15 values at T.N. -14^h to T.N. $+14^h$ are found, and the values $\bar{D}(\nu)$ where ν is an index starting with 1 at T.N. -14^h can be computed from

$$\bar{D}(\nu) = a_0(\nu-1) + \sum_{k=1}^{7}\left[a_k \sin\left(\frac{2\pi}{15}(\nu-1)k\right) + b_k\left\{1-\cos\left(\frac{2\pi}{15}(\nu-1)k\right)\right\}\right] \Big/ \frac{2\pi k}{15}. \tag{7}$$

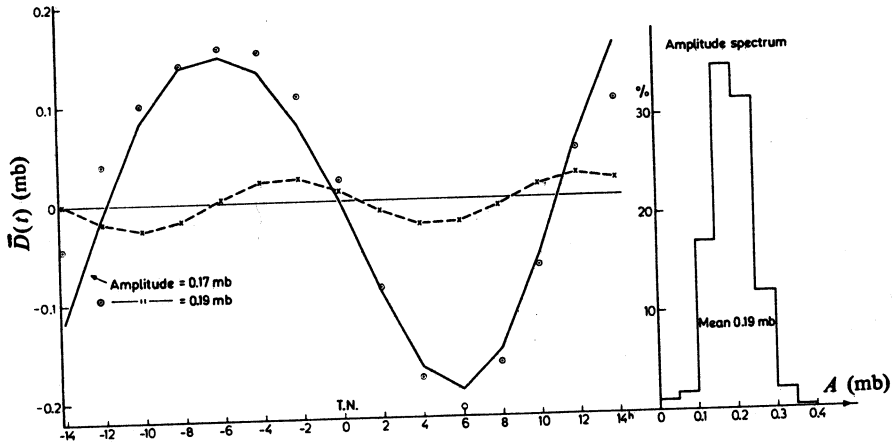

Fig. 8. Dynamic mean pressure variation where the solid curve shows the result obtained by means of formula (7) and the crosses the first harmonic. The circles show a mean curve obtained from the series $D(t)$. In the right part the amplitude spectrum of $D(t)$ is shown.

In Fig. 8 the solid curve shows the result. A maximum occurs 6 hours before T.N. and a minimum 6 hours after T.N., with the pressure decreasing fastest when the tidal acceleration has its largest value. The mean amplitude is 0·17 mb. The Fourier method also facilitates a study of the harmonics. Crosses and the dashed curve show the first harmonic with a period of 14 hours. Its amplitude is 0·02 mb, and the second harmonic has an amplitude of 0·01 mb. The first method results in the mean curve indicated by circles. Again the method which was used to find the series $D(t)$ has been confirmed. In the right part of Fig. 8 the amplitude spectrum A of $D(t)$ is shown. The mean amplitude is 0·19 mb, but it is interesting that amplitudes up to 0·35 mb are present in 2% of the cases.

8. Thermal Contribution

Fig. 4*d* shows the gradient of the pressure when the data are grouped with a period of 24 hours or a solar day. The curve showing the variation during a solar day represents a mean of 13 years, and it has been denoted by $\bar{T}'(\nu)$ where $\nu = 1, 2, ..., 13$ correspond to $0^h, 2^h, ..., 24^h$ CET. Of course there is a high degree of dependence upon the season. In order to separate this effect the statistics were divided into 12

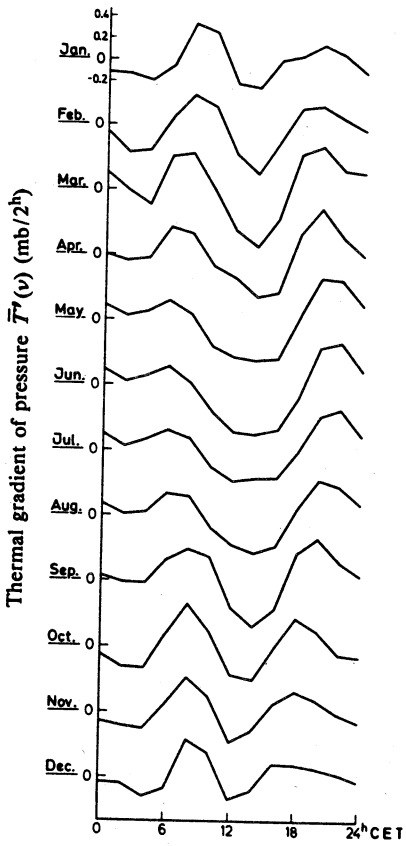

Fig. 9. Thermal gradient of the pressure showing the mean daily variations for each month.

groups containing the results for each month. Then, mean values for 13 months of January, 13 months of February etc. were formed. Fig. 9 shows the result. There are two maxima and two minima each day, most pronounced during the winter months.

The next step was to use the results to form a continuous series covering every day of the year by linear interpolation. This series may be designated by $T'(t)$ where $t = 1, 2, \ldots, 4380$ starting with 1 at January 1st 0^h. Then integration is performed by means of the trapezoidal formula to form the series

$$T(t) = \int_0^t T'(x)\,\mathrm{d}x.$$

Again the same test as before was performed. The series $T(t)$ was substituted for the observed data and a new curve for the mean gradient $\bar{T}'(\nu)$ found. In Fig. 10*a* the result is seen. The original curve is shown, the same as shown in Fig. 4*d*, while the crosses show the result with $T(t)$ as data. Once more the mean value of the function $T(t)$ can be found in two ways, either by summing values from the same hour in the series, or by integrating the function $\bar{T}'(\nu)$ which had been obtained directly from the data. A trigonometric interpolation formula was defined, exactly as given in Section 7, and the curve in Fig. 10*b* shows the result. The crosses correspond to those in (*a*) where the series $T(t)$ was used as the data. Finally, the circles represent

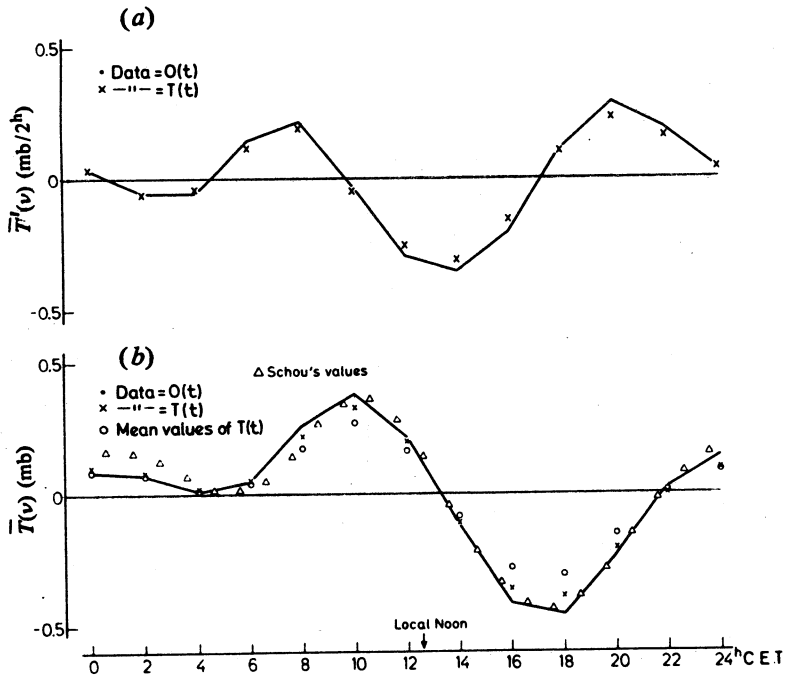

Fig. 10. Thermal daily variation: (*a*) The curve shows the yearly mean gradient $\bar{T}'(\nu)$ determined from the original data (the same curve as shown in Fig. 4*d*) and the crosses show the result with the series $T(t)$ as the data. (*b*) The integrated mean function $\bar{T}(\nu)$ based upon the original data is shown by the curve. Crosses show the result when the series $T(t)$ is used as the data, and the triangles show Schou's (1939) result.

the result of summing all values in $T(t)$ corresponding to the same solar hour and forming mean values. We note that the amplitude of the curves defined by the crosses and by the circles is smaller than the solid curve. A possible explanation of this fact will be given in Section 10 where the correlation between the series $T(t)$ and $D(t)$ is discussed.

In Table 1 the monthly means of the function $T(t)$ are shown every second hour from 0^h to 22^h CET.

9. Thermal Oscillation Compared with Earlier Results

Schou (1939) presented tables of the pressure for every hour local time at a number of stations in Norway. The table for Oslo is based on observations during the 40 year period 1893–1932. The monthly mean of the daily pressure variation normalised to the mean pressure of the month is given for every hour local time. The presentation is therefore similar to Table 1, the only difference being that Schou used local time. The measurements used by him were obtained in Oslo 24·9 m above sea level, whereas the present observations were obtained 3·5 km further north at an altitude of 96 m. Therefore, the results of Schou prepared by the classical method should constitute an independent test of the method used here. From Schou's Table 2 (p. 37) values

Table 1. Monthly means of the daily pressure variation $T(t)$

H	Jan.	Feb.	Mar.	Apr.	May	Jun.	Jul.	Aug.	Sep.	Oct.	Nov.	Dec.
0	0·100	0·155	0·164	0·111	0·105	0·082	0·122	0·079	0·102	0·084	0·113	0·116
2	−0·002	0·064	0·170	0·100	0·186	0·192	0·183	0·116	0·075	−0·031	0·001	0·033
4	−0·153	−0·119	0·051	0·059	0·243	0·279	0·222	0·119	0·009	−0·197	−0·152	−0·107
6	−0·260	−0·159	0·087	0·160	0·380	0·436	0·338	0·217	0·054	−0·221	−0·215	−0·248
8	−0·103	0·054	0·346	0·372	0·517	0·567	0·464	0·394	0·268	0·026	−0·033	−0·127
10	0·201	0·308	0·473	0·405	0·445	0·497	0·415	0·419	0·399	0·276	0·200	0·142
12	0·228	0·279	0·279	0·216	0·169	0·209	0·162	0·214	0·254	0·211	0·136	0·131
14	−0·001	−0·047	−0·161	−0·114	−0·184	−0·175	−0·155	−0·113	−0·098	−0·069	−0·100	−0·065
16	−0·123	−0·306	−0·557	−0·488	−0·549	−0·548	−0·462	−0·442	−0·435	−0·231	−0·167	−0·103
18	−0·078	−0·270	−0·567	−0·571	−0·707	−0·752	−0·628	−0·558	−0·461	−0·115	−0·042	−0·004
20	0·040	−0·063	−0·265	−0·276	−0·491	−0·592	−0·492	−0·366	−0·198	0·098	0·107	0·090
22	0·151	0·103	−0·021	0·127	−0·113	−0·194	−0·168	−0·079	0·029	0·169	0·153	0·142

for $0^h, 2^h, ..., 22^h$ were selected in order to make them compatible with our data. The yearly mean is formed from the monthly values, and the harmonic components are computed. If $S_1(\tau)$ and $S_2(\tau)$ represent the one-day and half-day components respectively, we get

$$S_1(\tau) = 0{\cdot}249 \sin(\tau + 3{\cdot}8), \qquad S_2(\tau) = 0{\cdot}224 \sin(2\tau + 133{\cdot}4), \tag{8}$$

where τ denotes local time measured in degrees ($1^h = 15°$) from midnight, the unit being millibar. Similarly, separation of the mean function $\bar{T}(\nu)$ into its harmonic components $\bar{T}_1$ and $\bar{T}_2$ and introduction of local time, which is $4°{\cdot}28$ less than CET, results in

$$\begin{aligned} \bar{T}_1(\tau) &= 0{\cdot}287 \sin(\tau - 4{\cdot}9) & \bar{T}_2(\tau) &= 0{\cdot}219 \sin(2\tau + 131{\cdot}5) \\ &= 0{\cdot}236 \sin(\tau - 5{\cdot}0) & &= 0{\cdot}188 \sin(2\tau + 131{\cdot}8) \\ &= 0{\cdot}240 \sin(\tau - 5{\cdot}0), & &= 0{\cdot}199 \sin(2\tau + 131{\cdot}7), \end{aligned} \tag{9}$$

where the three functions $\bar{T}(\nu)$ from Fig. 10*b* are shown in the same order. There is a difference of $8°{\cdot}8$ between the phase constants of S_1 and $\bar{T}_1$, corresponding to 35 minutes, but the phase constants of S_2 and $\bar{T}_2$ are nearly equal. If we consider the different methods used and the different datasets, it may be concluded that the agreement is satisfactory. In Fig. 10*b* where the curve shows the mean function $\bar{T}(\nu)$, Schou's values are marked by triangles.

10. Connection between the Dynamic and Thermal Effect

Having found the two series, $T(t)$ representing the thermal tide, and $D(t)$ which is of dynamic origin, it is tempting as a final test to subtract both of them from the original data series $O(t)$. Then, this new series could be used as the data in the programs which determined the mean gradients $\bar{T}'(\nu)$ and $\bar{D}'(\nu)$ and we might expect to obtain results close to zero. But this did not happen. In both attempts the data had been more than compensated, resulting in gradients running opposite to the former curves of Figs 4*a* and 4*d*. The explanation is already indicated in Section 1. Every month there will be a few days when the thermal and dynamic effects operate in unison. In Fig. 7 it was demonstrated that the correlation coefficient between the gradient of the pressure and the magnitude of the tidal acceleration during a tidal day showed a different behaviour if the series $D(t)$ instead of $O(t)$ was used as the data.

Now the same program can be run with $T(t)$ as the data, and we find a correlation coefficient showing two maxima and two minima as indicated in Fig. 11, where the correlation coefficients for the three cases are placed together and the curves marked *O*, *D* and *T*. When looking at Fig. 11 a natural idea would be that the two series $D(t)$ and $T(t)$ are also correlated. But this is not the case. The correlation coefficient between the two series was computed and the result was zero in the statistical sense. The mean value for all of the years was smaller than the standard deviation; actually the result was $-0{\cdot}035 \pm 0{\cdot}043$. The correlation coefficients shown in Fig. 11 can be used to construct two factors a and b such that the dataset $O(t) - aT(t) - bD(t)$ will

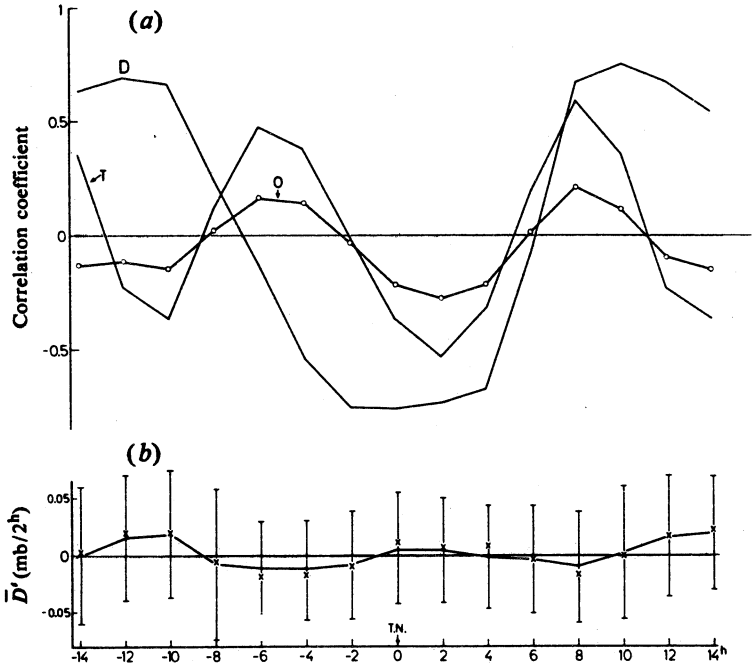

Fig. 11. (*a*) Correlation coefficient between the dynamic gradient and the magnitude of the acceleration with the three datasets $O(t)$, $D(t)$ and $T(t)$. (*b*) Residual dynamic gradient where the curve is for dataset $O(t) - 0{\cdot}355\ T(t) - 0{\cdot}613\ D(t)$ and crosses for dataset $O(t) - D(t)$.

produce almost no gradient of the pressure. From the curves marked T and D in Fig. 11*a* the mean square deviations may be formed to give $a = 0{\cdot}355$ and $b = 0{\cdot}613$ respectively. Then with the dataset $O(t) - 0{\cdot}355\ T(t) - 0{\cdot}613\ D(t)$, the dynamical gradient $\bar{D}'(\nu)$ shown in Fig. 11 *b* by the curve is obtained. The uncertainty is shown by the vertical bars. Crosses mark the former result where the series $O(t) - D(t)$ had been used. It is obvious that the result is zero in the statistical sense, and it is immaterial whether the series $D(t)$ or the combination $aD(t) + bT(t)$ is subtracted from the data.

Now since there is a significant correlation between the gradient and the magnitude of the acceleration when the series $T(t)$ is used as the data, it might be suspected that conversely we could find a significant variation within the solar day if the series $D(t)$ is used as the data. This did not happen. Instead the deviations of $\bar{T}'(\nu)$ from zero became smaller than $0{\cdot}005$ mb/2^h, independent of the time of day. This of course is consistent with the fact that the two series $T(t)$ and $D(t)$ are uncorrelated. It proves again that the dynamic wave represented by $D(t)$ can only be explained by the lunisolar tide.

However, it is interesting that the thermal variation $T(t)$ alone will produce oscillations during the tidal day. An explanation may be that the dynamic wave acts upon the thermal wave as a feedback system for some days every fortnight, meaning that part of the series $T(t)$ actually is of dynamic origin.

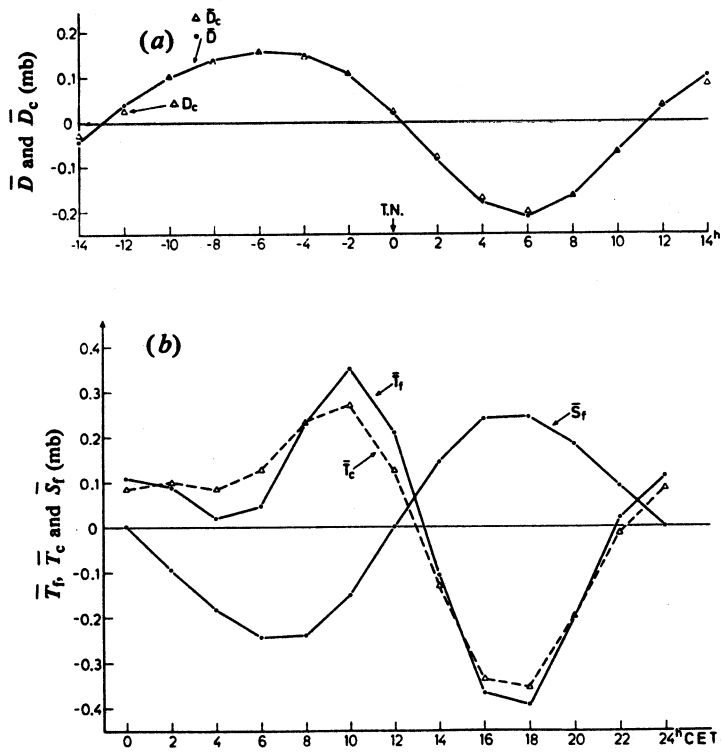

Fig. 12. (*a*) Mean dynamic pressure variation during the tidal day, $\bar{D}(\nu)$, shown by the curve, and the corrected mean $\bar{D}_c(\nu)$, shown by triangles. (*b*) Filtered mean daily thermal variation $\bar{T}_f(\nu)$ and the filtered daily variation of the thermal balance function $\bar{S}_f(\nu)$ both shown by solid curves. The triangles (dashed curve and indicated by $\bar{T}_c$) give the mean daily variation of the corrected thermal series $T_c(t)$.

11. Multicorrelation Analysis

Since the series $D(t)$ of dynamic origin is significantly correlated with the magnitude of the acceleration, an attempt was made to find a function which would be correlated with the thermal series $T(t)$. For that purpose a function which describes the radiative balance of the atmosphere was defined. First the accumulated insolation $\int_{-H_0}^{H} \cos z \, dH$ was computed, where H is the hour angle of the Sun, H_0 its value at sunset and z is the zenith distance as given by formula (3). The integration started on January 1st at sunrise was continued the next day from sunrise to sunset through the year, and its value every 2^h was noted. In the course of a year the same amount has to be radiated into space at a constant rate, day and night. The series $S(t)$ which is the accumulated insolation minus the radiation was computed and listed every 2^h. Strictly speaking $S(t)$ should be multiplied by the solar constant, but this has been omitted because the purpose is only to use correlation coefficients, which are independent of the scale. The first attempt to correlate $S(t)$ and $T(t)$ resulted in a correlation coefficient 0·24, almost independent of the time of day. This only reflects the fact that both series show a dominant yearly variation. In order to study the daily variations, periods longer than 24^h were removed from $S(t)$ and $T(t)$ by a filtering method similar to the previous one described in Section 2, but this time covering 4380

or 4392 datapoints. In Fig. 12*b* the yearly means of the filtered series $T_f(t)$ and $S_f(t)$ are shown as functions of the time of day. The curve $\bar{T}_f$ does not differ much from $\bar{T}$ shown in Fig. 10*b*, but the shape of $\bar{S}_f$ is interesting. Small values of $\bar{S}_f$ result in increasing pressure and vice versa. Most important is the numerically high value of the correlation coefficient of $-0{\cdot}819$ between the two series $S_f(t)$ and $T_f(t)$.

Having obtained this promising result, we performed a multicorrelation analysis between four functions:

(1) F, the magnitude of the tidal acceleration (one value each tidal day);

(2) S_f, the filtered daily variation of the radiative balance;

(3) T_f, the filtered thermal series $T(t)$; and

(4) D, the dynamical variation of the pressure.

The sampling had to be chosen according to the tidal day, and for every value of the tidal phase ν the analysis had to be repeated, giving 15 separate results. The absolute correlation coefficients $r_{12}, r_{13}, r_{14}, r_{23}, r_{24}, r_{34}$ were computed, the determinant

$$\Delta = \begin{vmatrix} 1 & r_{12} & r_{13} & r_{14} \\ r_{12} & 1 & r_{23} & r_{24} \\ r_{13} & r_{23} & 1 & r_{34} \\ r_{14} & r_{24} & r_{34} & 1 \end{vmatrix} \tag{10}$$

was formed, and its minors Δ_{ij} were computed. Further, the standard deviations $\sigma_1, \sigma_2, \sigma_3, \sigma_4$ were found and the coefficients

$$B_{ij} = -\sigma_i \Delta_{ij} / \sigma_j \Delta_{ii} \tag{11}$$

were determined. Then, the connection between the mean functions F, S_f, T_f and D becomes

$$\begin{aligned} T_f &= B_{31} F + B_{32} S_f + B_{34} D, \\ D &= B_{41} F + B_{42} S_f + B_{43} T_f. \end{aligned} \tag{12}$$

Since it is suggested that the functions F and S_f are the causes and T_f and D are the effects, solution of equations (12) leads to

$$\begin{aligned} T_c &= \{(B_{31} + B_{34} B_{41})F + (B_{32} + B_{34} B_{42})S_f\}/(1 - B_{34} B_{43}), \\ D_c &= \{(B_{41} + B_{43} B_{31})F + (B_{42} + B_{43} B_{32})S_f\}/(1 - B_{34} B_{43}), \end{aligned} \tag{13}$$

where T_c and D_c can be interpreted as corrected thermal and dynamical functions. The coefficients

$$\begin{aligned} C_{FT} &= (B_{31} + B_{34} B_{41})/(1 - B_{34} B_{43}), \\ C_{ST} &= (B_{32} + B_{34} B_{42})/(1 - B_{34} B_{43}), \\ C_{FD} &= (B_{41} + B_{43} B_{31})/(1 - B_{34} B_{43}), \\ C_{SD} &= (B_{42} + B_{43} B_{32})/(1 - B_{34} B_{43}), \end{aligned} \tag{14}$$

are listed in Table 2 as functions of the tidal phase ν.

Table 2. Multicorrelation coefficients

T.N.+	C_{FT}	C_{ST}	C_{FD}	C_{SD}	ν
−14	0·3074	−1·068	−0·1081	−0·0956	1
−12	0·2637	−1·101	0·0000	−0·1181	2
−10	−0·0500	−1·014	0·0694	0·0879	3
−8	−0·2844	−0·984	0·1023	0·0000	4
−6	−0·1955	−1·042	0·1185	0·0085	5
−4	0·0431	−1·047	0·1180	0·0528	6
−2	0·2265	−1·035	0·0795	0·0669	7
0	0·2082	−1·062	0·0000	0·0749	8
2	0·0157	−1·035	−0·0931	0·0727	9
4	−0·2477	−0·958	−0·1717	0·0203	10
6	−0·3077	−0·981	−0·1984	0·0091	11
8	−0·0288	−1·047	−0·1599	−0·0808	12
10	0·3060	−1·073	−0·0764	−0·1470	13
12	0·2637	−1·101	0·0249	−0·1410	14
14	−0·0490	−1·014	0·1046	−0·0754	15

Next, within the intervals where the tidal days were defined, the corrected series $T_c(t) = C_{FT} F + C_{ST} S_f$ and $D_c(t) = C_{FD} F + C_{SD} S_f$ were formed. In the intervals where the tidal days had not been defined, the values of $T_c(t)$ were set equal to $T_f(t)$ and $D_c(t) = 0$. Then, the grand means were formed again and Fig. 12 shows the results. In Fig. 12*a* the mean dynamical variation $\bar{D}(\nu)$ is shown by the curve and $\bar{D}_c(\nu)$ by triangles. The two are practically identical. However, in Fig. 12*b*, where $\bar{T}_f(\nu)$ is shown by the solid curve and $\bar{T}_c(\nu)$ by the dot–dash curve, two differences become apparent. Firstly, the amplitudes of $\bar{T}_c$ is diminished relative to that of $\bar{T}_f$, exactly as expected, and secondly the maximum at about 10^h seems to be displaced to the left, approximately one-half hour earlier.

In Table 3 the monthly means of the daily variation of the function $T_c(t)$ have been listed for every second hour from 0^h to 22^h CET.

12. Conclusions

In the foregoing every test confirms the existence of a lunisolar one-day atmospheric pressure oscillation with a mean amplitude of 0·17 mb. This comes into existence when the Moon has increasing numerical values of declination, it decreases again when the equator is approached, and so on. This is a consequence of the high latitude of the station (Oslo at 60° north). It may be compared with the values for the lunar half-day variations L_2 of Fig. 2L.6 in Chapman and Lindzen (1970). The amplitude of L_2 is extremely small in high latitudes, actually only 0·007 mb in Oslo. But in the tropics it reaches values of up to 0·080 mb. Probably the atmospheric dynamical tidal wave will appear in the one-day mode at every station, north or south, with high latitude.

In equatorial stations the one-day luni-solar oscillation cannot exist. When the latitude is close to zero, formula (4) shows that the magnitude of the tidal acceleration becomes equal at upper and lower culmination.

The curious fact that the thermal one-day oscillation has a small amplitude compared with its first harmonic, the half-day oscillation, is possibly explained by

Table 3. Monthly means of the corrected series $T_c(t)$

H	Jan.	Feb.	Mar.	Apr.	May	Jun.	Jul.	Aug.	Sep.	Oct.	Nov.	Dec.
0	0·045	−0·073	−0·112	−0·048	0·090	0·180	0·175	0·120	0·138	0·165	0·187	0·166
2	−0·042	−0·120	−0·050	0·082	0·193	0·200	0·136	0·096	0·175	0·218	0·208	0·116
4	−0·112	−0·108	0·035	0·150	0·200	0·173	0·134	0·150	0·192	0·154	0·085	−0·017
6	−0·035	0·076	0·193	0·226	0·215	0·193	0·235	0·281	0·218	0·065	−0·044	−0·082
8	0·207	0·327	0·385	0·309	0·271	0·281	0·344	0·356	0·234	0·065	−0·014	0·044
10	0·368	0·423	0·403	0·305	0·299	0·308	0·304	0·244	0·138	0·072	0·122	0·228
12	0·221	0·237	0·225	0·204	0·206	0·167	0·070	−0·035	−0·076	−0·021	0·120	0·188
14	−0·093	−0·087	−0·068	0·001	−0·016	−0·120	−0·248	−0·326	−0·306	−0·179	−0·063	−0·047
16	−0·281	−0·279	−0·308	−0·270	−0·321	−0·426	−0·487	−0·478	−0·409	−0·277	−0·229	−0·248
18	−0·245	−0·231	−0·332	−0·420	−0·526	−0·548	−0·488	−0·378	−0·306	−0·221	−0·264	−0·282
20	−0·083	−0·109	−0·217	−0·346	−0·448	−0·375	−0·235	−0·116	−0·076	−0·089	−0·151	−0·136
22	0·051	−0·056	−0·154	−0·193	−0·162	−0·033	0·059	0·085	0·078	0·046	0·042	0·068

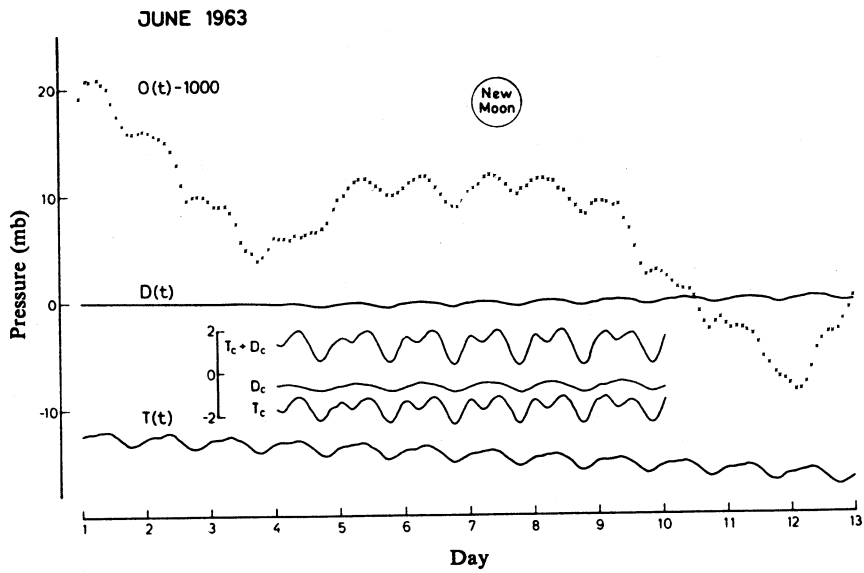

Fig. 13. Situation during the first half of June 1963. Crosses show the observed pressure values $O(t)$, while the dynamic variation $D(t)$ and the thermal variation $T(t)$ are shown by solid curves. During the interval between the 4th and the 10th the corrected series $D_c(t)$ and $T_c(t)$ together with the sum $T_c + D_c$ are shown using a doubled vertical scale.

the feedback of the dynamic tide, and the closeness to the natural frequency of the atmosphere.

As an illustration Fig. 13 shows the resulting curves $T(t)$ and $D(t)$ for the first half of June 1963. The crosses mark the observed pressure series. During the interval between the 4th and the 10th the corrected series $D_c(t)$ and $T_c(t)$ together with the sum $D_c + T_c$ are shown using a doubled vertical scale.

The Moon and the Weather. It may be relevant to raise the question again: does the Moon influence the weather? It is interesting to quote two papers, one by Bradley *et al.* (1962) and the other by Adderly and Bowen (1962). Together they found a clear correspondence between the phases of the Moon and precipitation during 50 years in the USA and 25 years in New Zealand respectively (see Figs 14 and 15). Bradley *et al.* commented: 'The quantitative nature of the indicated lunation effect is clear from a separate plotting of the 185 dates which registered as precipitation maxima at ten or more stations. The amplitude of the diphasic 29·53 day cycle is remarkable, since the dates of the most extreme widespread rainfalls in the US history are three times more frequent during the cyclic peak periods than during the cyclic troughperiods.'

In view of the results presented here, it is tempting to suggest that the tidal pressure variations are causing these variations in precipitation.

Acknowledgments

I am grateful for the observational data of pressure measurements received from the Norwegian Meteorological Institute, and also for pressure data measured at Batavia in 1919 which I received from the Royal Netherlands Meteorological Institute.

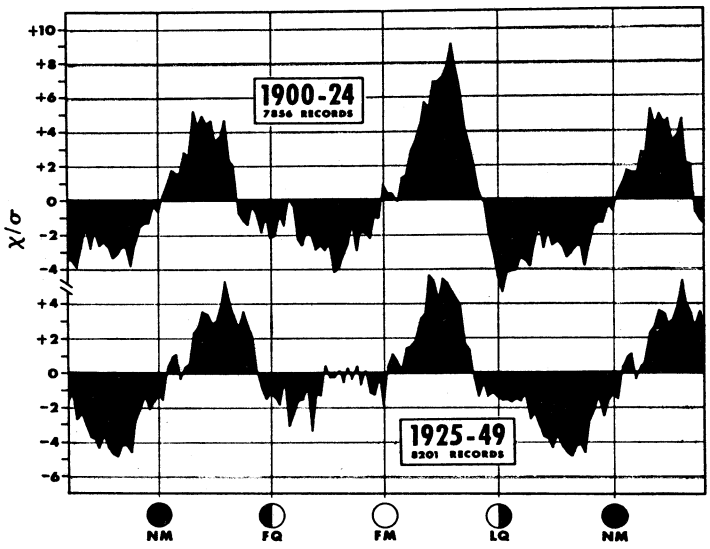

Fig. 14. Deviations (in terms of standard measure) of ten-unit moving totals of synodic decimals for 16,057 record dates of maximum 24-hour precipitation at 1544 US stations 1900–49, treated in separate 25 year series for correlative comparison. [From Bradley *et al.* (1962).]

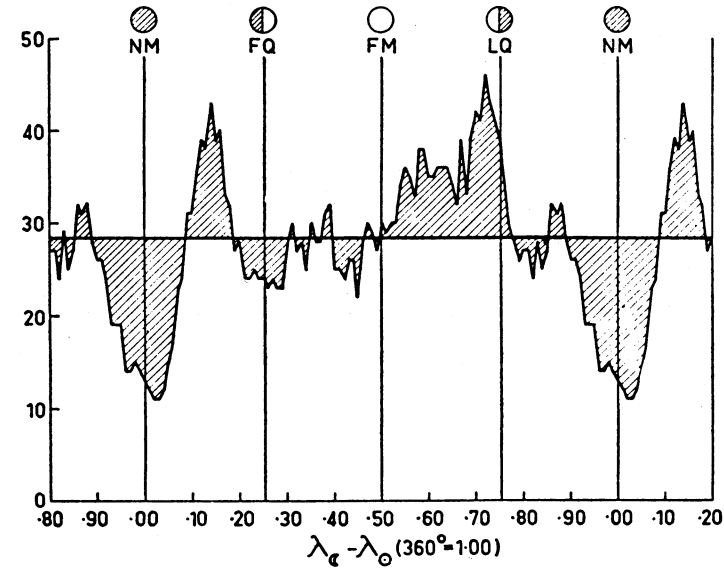

Fig. 15. Ten-unit moving totals of the heaviest falls of the month for 50 New Zealand stations, for the years 1901–25, plotted against the synodic decimal. [From Adderly and Bowen (1962).]

References

Abramowitz, M., and Stegun, I. A. (1964). 'Handbook of Mathematical Functions' (National Bureau of Standards: Washington).
Adderly, E. E., and Bowen, E. G. (1962). *Science* **137**, 749–50.
Bradley, D. A., *et al.* (1962). *Science* **137**, 748–9.
Chapman, S., and Lindzen, R. S. (1970). 'Atmospheric Tides' (Reidel: Dordrecht).
Haurwitz, B., and Cowley, A. D. (1969). *Pure Appl. Geophys.* **6**, 122–50.
Malin, S. R. C., and Chapman, S. (1970). *Geophys. J. R. Astron. Soc.* **19**, 15–35.
Meeus, J. (1962). 'Tables of Moon and Sun' (Kessel-Lo: Belgium).
Schou, G. (1939). *Geophys. Publ.* **14**, No. 2.

Manuscript received 9 October 1985, accepted 31 May 1988